Supporting Information

Efficient purification of C_2H_2 from C_2H_2/CO_2 mixtures in an acid-base resistant metal-organic framework

Ling Zhang,[‡a] Ke Jiang,[‡a] Libo Li,[b,c] Yu-Pei Xia,[d] Tong-Liang Hu,[d] Yu Yang,[a] Yuanjing Cui,[a] Bin Li,*[a] Banglin Chen*[a,c] and Guodong Qian*[a]

[a] *State Key Laboratory of Silicon Materials, Cyrus Tang Center for Sensor Materials and Applications, Department of Materials Science & Engineering, Zhejiang University, Hangzhou 310027, China. E-mail: bin.li@zju.edu.cn; gdqian@zju.edu.cn.*

[b] *College of Chemistry and Chemical Engineering, Taiyuan University of Technology, Taiyuan, Shanxi 030024, P. R. China*

[c] *Department of Chemistry, University of Texas at San Antonio, One UTSA Circle, San Antonio, Texas 78249-0698, USA. E-mail: banglin.chen@utsa.edu; Fax: (+1) 210-458-7428.*

[d] *School of Materials Science and Engineering, NanKai University. 38 Tongyan Road, Haihe Education Park, Tianjin 300350, P.R.China.*

1. Materials and methods

All reagents and solvents were commercially available and used without further purification. Infrared spectrum (IR) was performed on Thermo Fisher Nicolet iS10 spectrometer using KBr pallets. Thermogravimetric analyses (TGA) were carried out on a Netzsch TG209F3 with a heating rate of 10°C/min in N_2 atmosphere. Elemental analyses for C, H, and N were performed on an EA1112 microelemental analyzer. Powder X-

ray diffraction (PXRD) patterns were collected in the 2θ = 3-50° range on an X'Pert PRO diffractometer with Cu Kα (λ = 1.542Å) radiation at room temperature.

2. Single-crystal X-ray crystallography.

Crystallographic measurements for **ZJU-196** were taken on a Rigaku XtaLAB MM007 CCD diffractometer at 100K with Cu Kα radiation (λ = 1.5418 Å) radiation. The determination of the unit cell and data collection for the crystal of **ZJU-196** was performed with CrysAlisPro. The structure of **ZJU-196** was determined by direct methods and refined by the full-matrix least-squares method with the SHELX program package. The solvent molecules in the compound are highly disordered. The SQUEEZE subroutine of the PLATON software suit was used to remove the scattering from the highly disordered guest molecules. The new resulting files were used to further refine the structure. The composition of the as-synthesized **ZJU-196** was figured out based on the elemental analysis, TGA and single crystal structure. Crystallographic data are summarized in Table S2.

3. Gas Sorption Measurements.

All gas sorption isotherms were obtained from the Micromeritics ASAP 2020 surface area analyzer. Before the gas sorption measurements, the collected crystal material was washed with fresh DMF for several times taking about half day to wipe off the residuum. The guest molecules within the framework could be exchanged successively by acetone for about 5 times taking about one day and by anhydrous dichloromethane for about 10 times taking about two days. After solvent-exchange, the crystal materials were evaluated at 273 K for 1 d and at room temperature for 1 d respectively to yield the activated **ZJU-196a**. The measurements were maintained at 196 K with drikold. An ice-water bath and water bath were used for C_2H_2 and CO_2 gases adsorption isotherms at 273 K and 298 K, respectively.

4. Synthesis of ZJU-196.

A mixture of the organic linker 3-amino-4-hydroxy benzoic acid (10 mg, 0.065 mmol) and $Zn(NO_3)_2 \cdot 6H_2O$ (15.0 mg, 0.068 mmol) was dissolved into a 2.7 mL

mixed solvent (DMF/H_2O/acetonitrile/alcohol, 2 mL/0.1 mL/0.3 ml/0.3 ml) in a screw-capped vial (20 mL), at 85°C for 3 d. Rod-shaped flaxen crystals were obtained as **ZJU-196**. **ZJU-196** has an assumed formula as ZnL·DMF·H_2O, which was obtained based on the single-crystal X-ray structure determination, elemental analysis (EA) and TGA. EA: calcd: $C_{10}H_{13}N_2O_5Zn$, found: C, 39.99; H, 4.02; N, 8.86; C, 40.02; H, 3.98; N, 8.89. TGA data for loss of DMF and H_2O: calcd: 29.6%, found: 25.3%.

5. Virial Graph Analysis

Estimation of the isosteric heats of gas adsorption (Qst)

A virial-type expression of comprising the temperature-independent parameters a_i and b_j was employed to calculate the enthalpies of adsorption for C_2H_2 (at 273 K and 298 K) on **ZJU-196a**. In each case, the data were fitted use equation:

$$\ln P = \ln N + 1/T \sum_{i=0}^{m} a_i N_i + \sum_{j=0}^{n} b_j N_j \qquad (1)$$

Here, P is the pressure expressed in Pa, N is the amount absorbed in mmol g^{-1}, T is the temperature in K, a_i and b_j are virial coefficients, and m, n represent the number of coefficients required to adequately describe the isotherms (m and n were gradually increased till the contribution of extra added a and b coefficients was deemed to be statistically insignificant towards the overall fit. And the average value of the squared deviations from the experimental values was minimized). The values of the virial coefficients a_0 through a_m were then used to calculate the isosteric heat of absorption using the following expression:

$$Q_{st} = -R \sum_{i=0}^{m} a_i N_i \qquad (2)$$

Qst is the coverage-dependent isosteric heat of adsorption and R is the universal gas constant. The heat enthalpy of C_2H_2 sorption for **ZJU-196a** in this manuscript is determined by using the sorption data measured in the pressure range from 0-1 bar (at 273 K and 298 K).

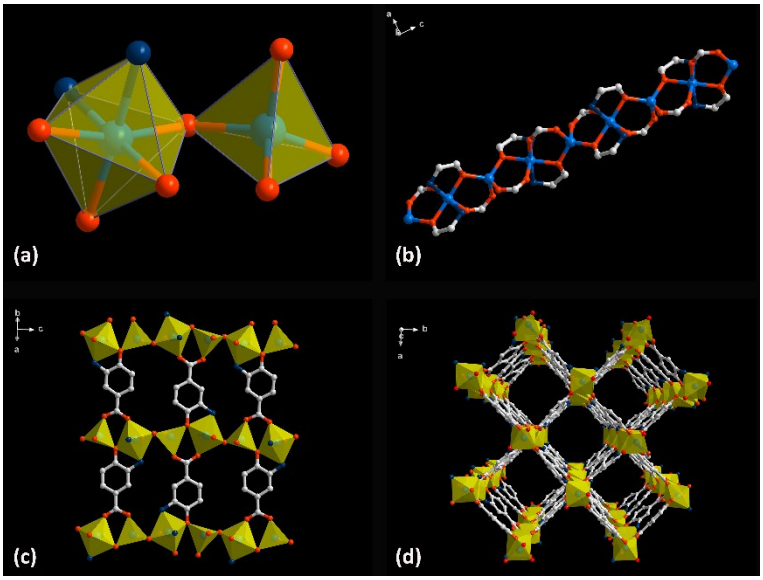

Figure S1. X-ray single crystal structure of **ZJU-196**, indicating that (a) there are two types SBUs of octahedron SBU and tetrahedron SBU; (b) the SBUs chains along c axis; (c) the 3D framework; (d) the 1D pore channels of about 5.1 Å × 5.1 Å viewed from c axis (C, white; O, red; Zn, blue; N, navy; H atoms are omitted for the clarity).

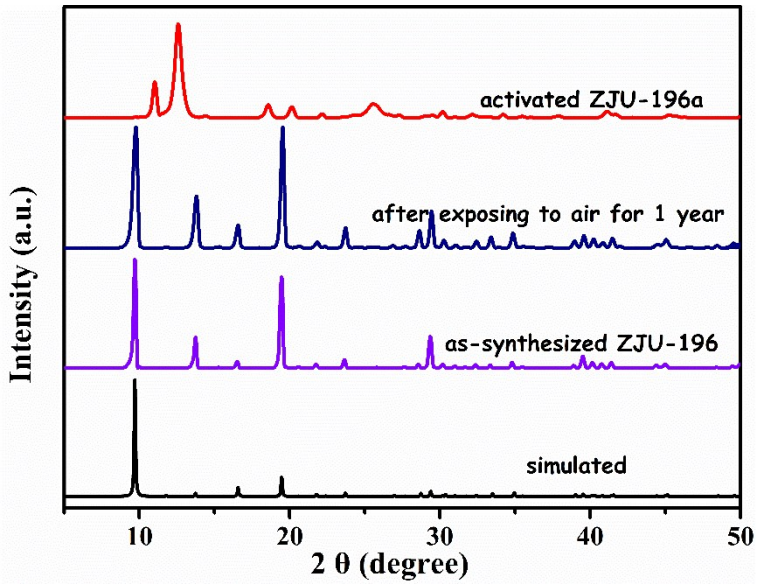

Figure S2. Powder X-ray diffraction (PXRD) patterns for as-synthesized **ZJU-196** (violet), **ZJU-196** after exposing air for 1 year (blue), activated **ZJU-196a** (red), along with the simulated XRD pattern from the single-crystal X-ray structure (black).

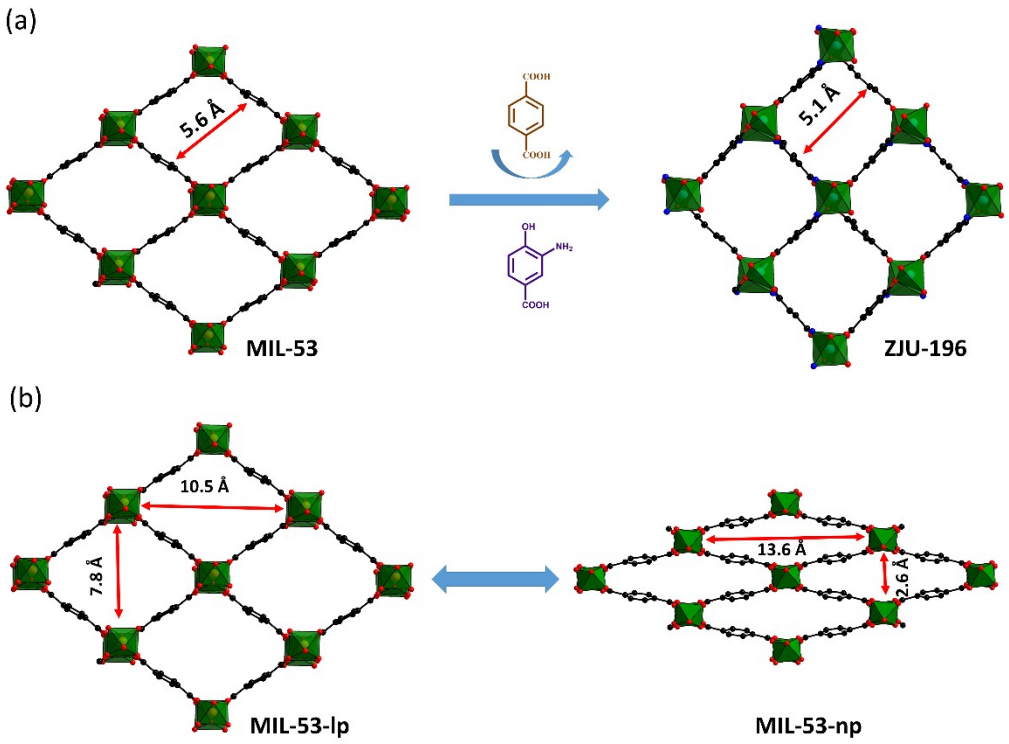

Figure S3. (a) Crystal structure of MIL-53 and **ZJU-196**, clearly indicating that **ZJU-196** has very similar structure and 1D rhombus-shaped channels with the well-known flexible MIL-53. (b) The structure change between MIL-53-lp with larger-pores and MIL-53-np with narrow pores.[1-4]

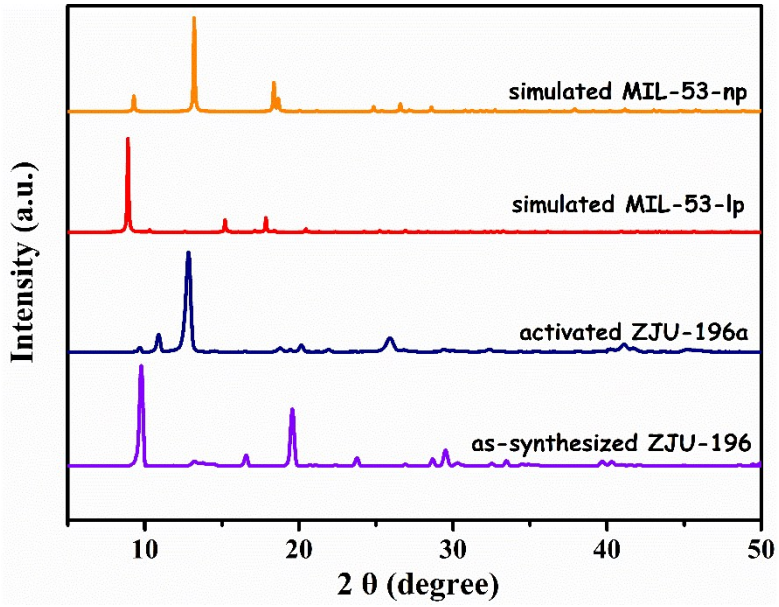

Figure S4. Comparison of the changes of PXRD patterns between **ZJU-196** and MIL-53, indicating that **ZJU-196** should have the similar pore transformation with MIL-53 from the

large-pore in **ZJU-196** switched to the small-pore in **ZJU-196a** after removing the guest molecules.

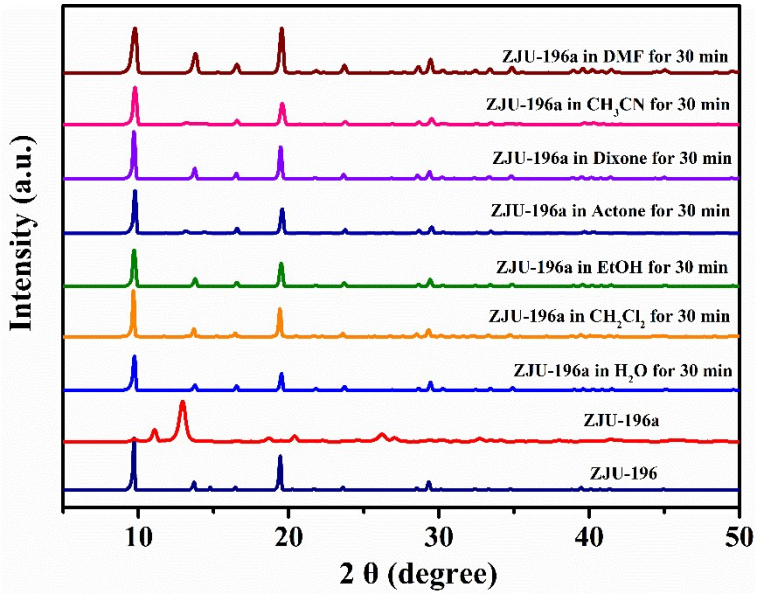

Figure S5. Powder X-ray diffraction (PXRD) patterns for activated **ZJU-196a** after soaking in different solvents for 30 minutes.

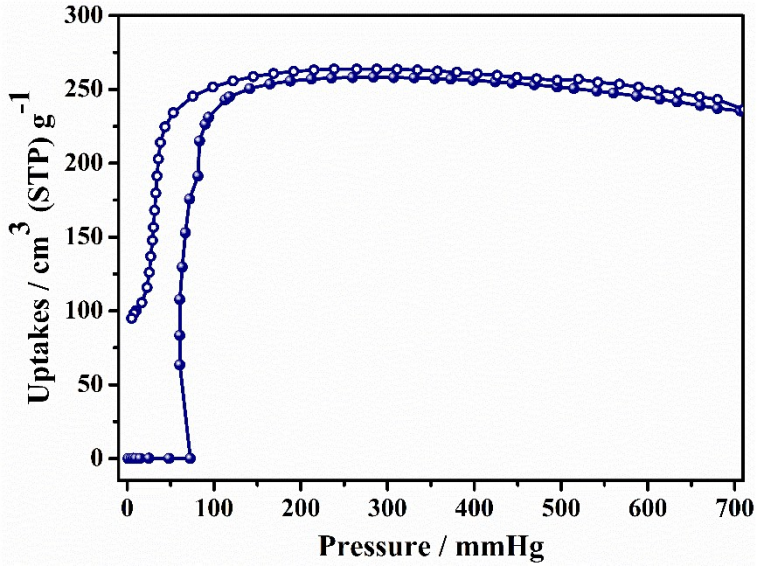

Figure S6. The CO_2 adsorption isotherms for **ZJU-196a** at 196 K.

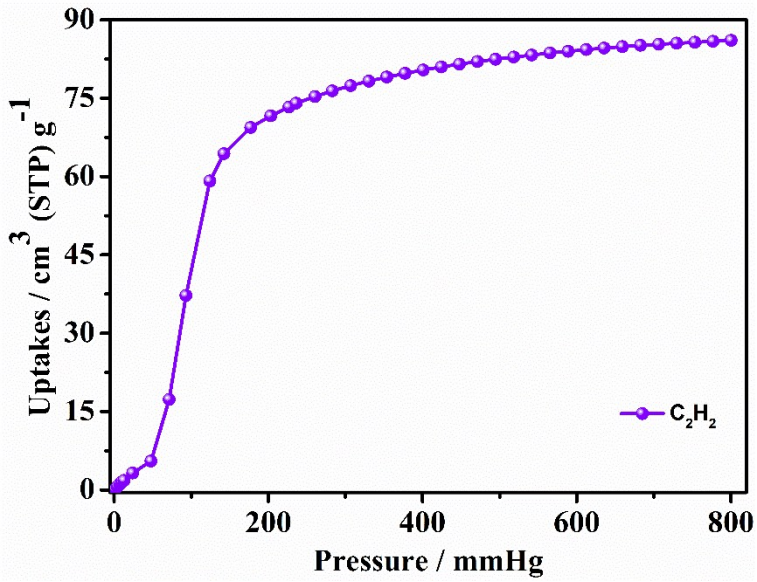

Figure S7. Single-component adsorption isotherm for C_2H_2 of **ZJU-196a** at 273 K.

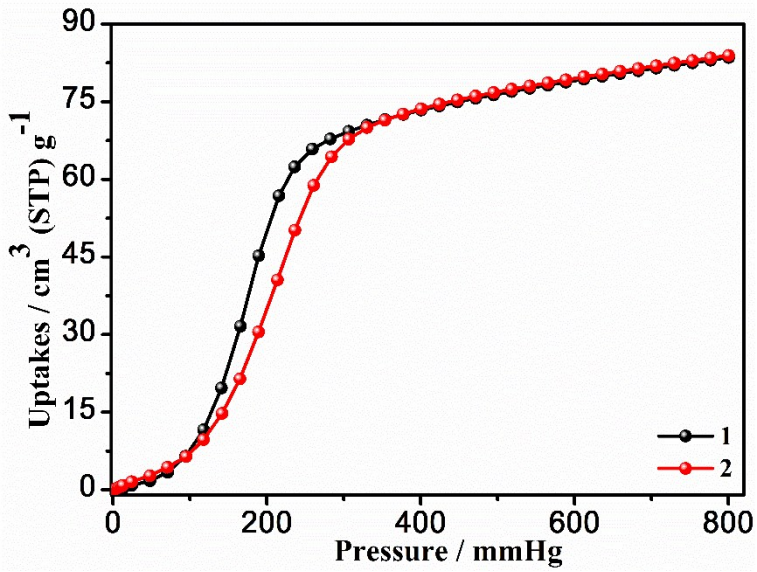

Figure S8. The C_2H_2 adsorption isotherms s at 298 K of the fresh activated **ZJU-196a** (**1**) and **ZJU-196a** after air exposure (70% humidity) for one year (**2**).

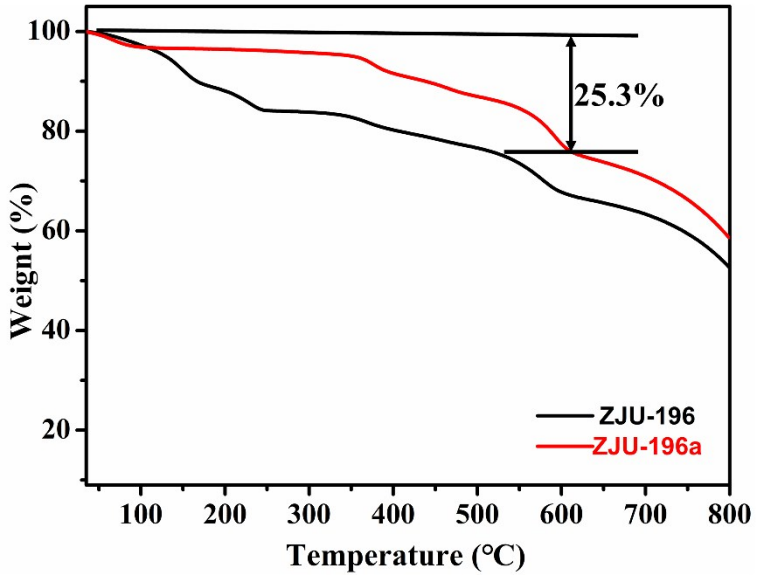

Figure S9. Thermogravimetric analysis (TGA) curves of as-synthesized **ZJU-196** and **ZJU-196a**. It's demonstrated the remarkable thermostability of **ZJU-196**, with no decomposition of framework occurring up to at least 500°C.

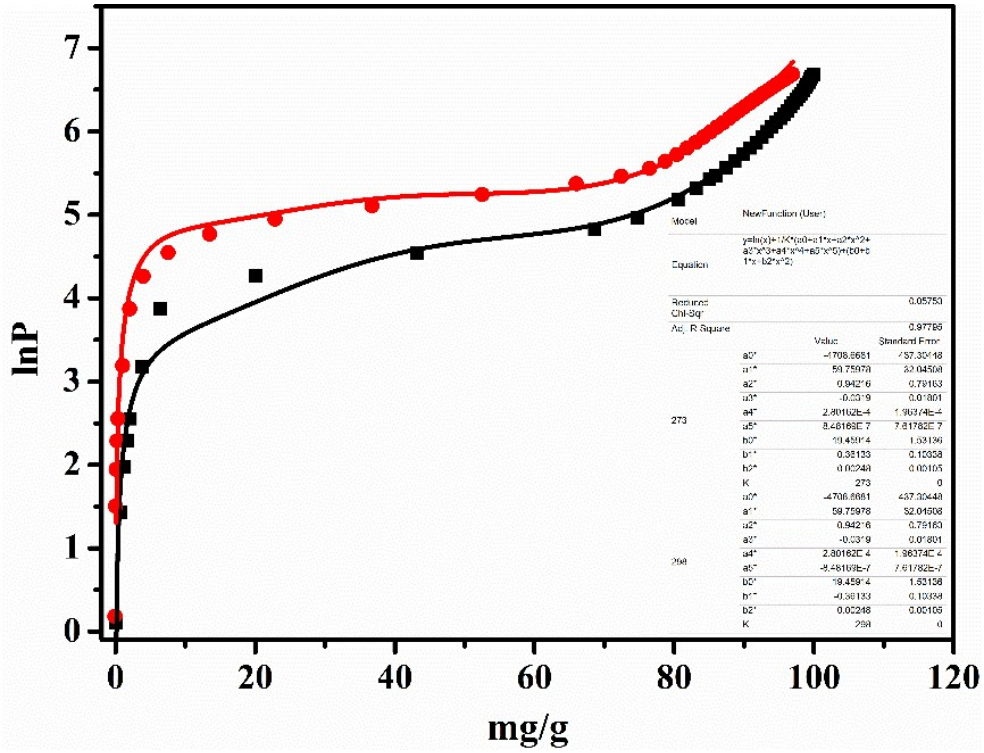

Figure S10. Virial fit parameters for C_2H_2.

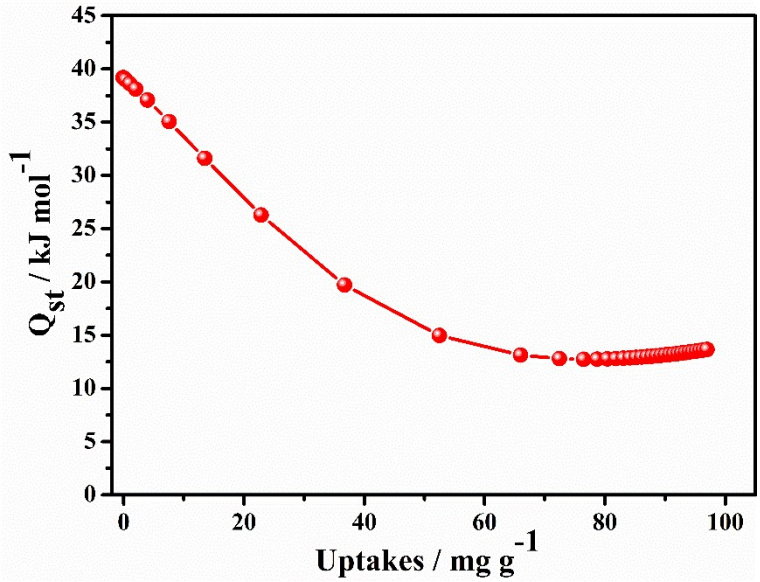

Figure S11. The isosteric heat of C_2H_2 adsorption (Qst) in **ZJU-196a**.

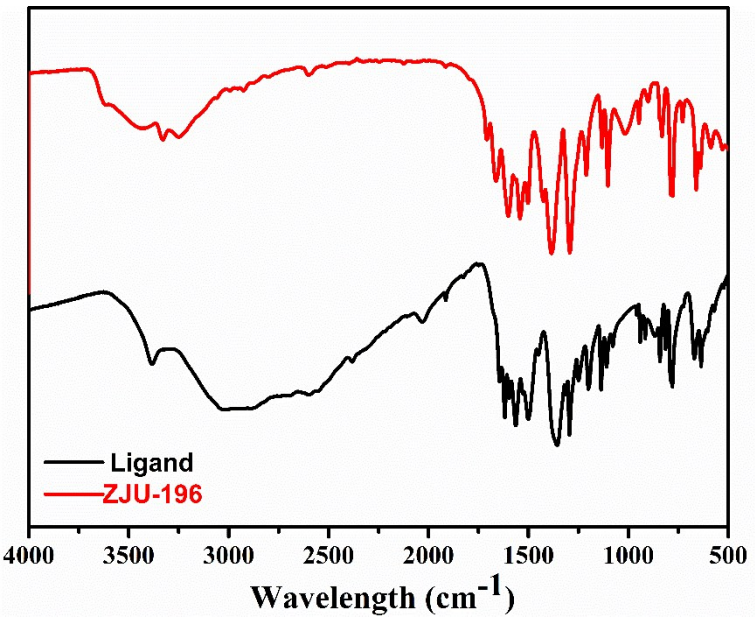

Figure S12. Infrared spectrum (IR) curves of ligand and as-synthesized **ZJU-196**.

6. Breakthrough test of ZJU-196.

Before the breakthrough test, **ZJU-196a** has to be pelleted due to the under-size items (Fig. S13). The breakthrough experiments were accomplished by a dynamic gas breakthrough equipment.[5,6] The experiment was conducted using a stainless steel column (4.0 mm inner diameter × 60 mm). The weight of sample powder packed in the column was 0.87 g. The column packed with sample was firstly activated with He flow (15 ml min^{-1}) for 12 h at 298 K and 273 K.

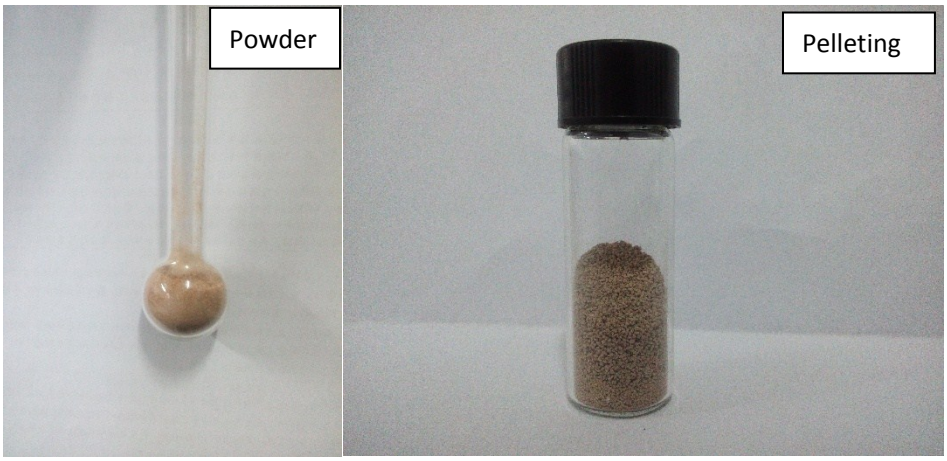

Figure S13. The powder of activated **ZJU-196a** and **ZJU-196a** after pelleting.

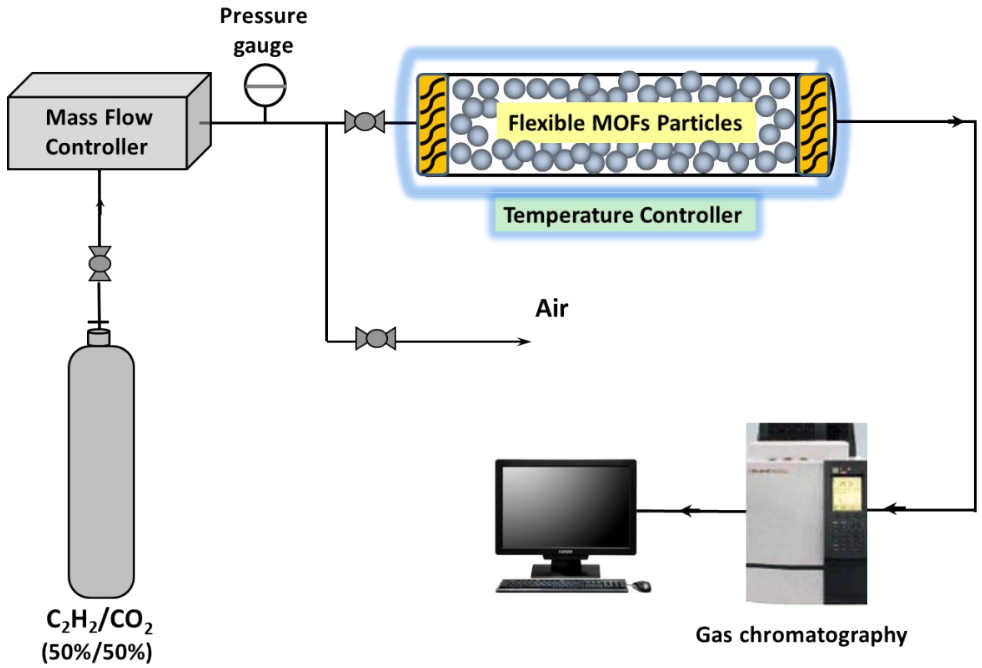

Figure S14. The equipment for the breakthrough test of **ZJU-196a**.

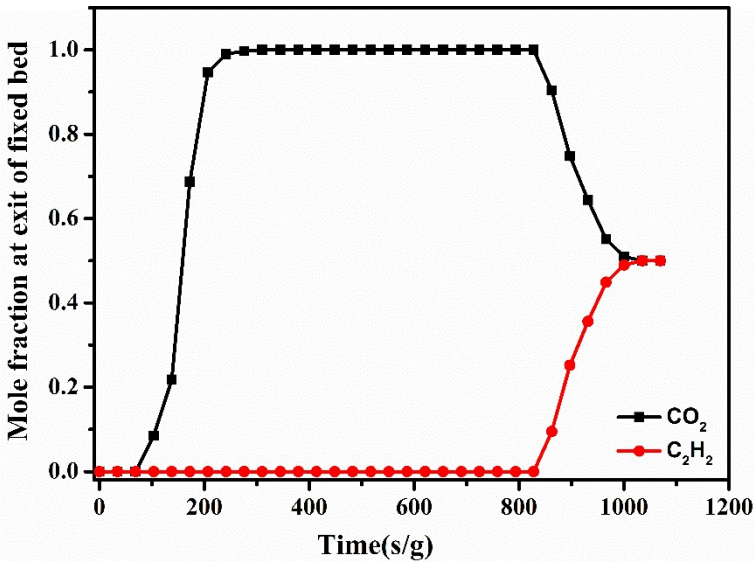

Figure S15. The breakthrough curves of **ZJU-196a** for the C_2H_2/CO_2 (50:50; v:v) separation at 273 K.

Table S1. The detail of the SQUEZE analysis of **ZJU-196.**

```
# SQUEEZE RESULTS (Version = 21116)
# Note: Data are Listed for all Voids in the P1 Unit Cell
# i.e. Centre of Gravity, Solvent Accessible Volume,
# Recovered number of Electrons in the Void and
# Details about the Squeezed Material
loop_
   _platon_squeeze_void_nr
   _platon_squeeze_void_average_x
   _platon_squeeze_void_average_y
   _platon_squeeze_void_average_z
   _platon_squeeze_void_volume
   _platon_squeeze_void_count_electrons
   _platon_squeeze_void_content
     1    0.000    0.000 -0.005          453          137 ' '
     2    0.500    0.500    0.847          493          133 ' '
_platon_squeeze_void_probe_radius                    1.20
_platon_squeeze_details                              ?
```

Table S2. Crystallographic data and structure refinement results for **ZJU-196**.

	ZJU-196
Empirical formula	$C_7H_4NO_3Zn$
Formula weight	215.48 g/mol
Temperature (K)	100.00(10)
Wavelength (Å)	1.54178 Å
Crystal system	Tetragonal
Space group	P 41 2 2
a (Å)	12.88630(10)
b (Å)	12.88630(10)
c (Å)	13.2102(3)
α (°)	90
β (°)	90
γ (°)	90
V ($Å^3$)	2193.64(6)
Z	8
Density (calculated g/cm^{-3})	1.305
Absorption coefficient (mm^{-1})	2.920
F(000)	856
GOF	1.090
R1, wR2 (I>2σ (I)) a	0.0372, 0.0955
R1, wR2 ((all data) a	0.0355, 0.0968
Largest diff. peak and hole ($e/Å^{-3}$)	1.296, -0.334

Reference

[1] T. Loiseau, C. Serre, C. Huguenard, G. Fink, F. Taulelle, M. Henry, T. Bataille and G. Ferey, *Chem. Eur. J.,* 2004, **10**, 1373-1382.

[2] P. L. Llewellyn, S. Bourrelly, C. Serre, Y. Filinchuk and G. Ferey, *Angew. Chem. Int. Ed.*, 2006, **45**, 7751-7754.

[3] S. Couck, J. F. M. Denayer, G. V. Baron, T. Remy, J. Gascon and F. Kapteijin, *J. Am. Chem. Soc.*, 2009, **131**, 6326-6327.

[4] F.-X. Coudert, M. Jeffroy, A. H. Fuchs, A. Boutin and C. Mellot-Draznieks, *J. Am. Chem. Soc.*, 2008, **130**, 14294-14302.

[5] L. Li, R. Krishna, Y. Wang, J. Yang, X. Wang and J. Li, *J. Mater. Chem. A*, 2016, **4**,751-755.

[6] L. Li, Y. Wang, J. Yang, X. Wang and J. Li, *J. Mater. Chem. A*, 2015, **3**, 22574-22583.